THYROID
Volume 29, Number 10, 2019
© Mary Ann Liebert, Inc.
DOI: 10.1089/thy.2018.0526

Increased Anaplastic Lymphoma Kinase Activity Induces a Poorly Differentiated Thyroid Carcinoma in Mice

Hannah Kohler,[1,*] Soeren Latteyer,[1,*] Georg Sebastian Hönes,[1] Sarah Theurer,[2] Xiao-Hui Liao,[3] Sandra Christoph,[4] Denise Zwanziger,[1] Johannes H. Schulte,[5] Jukka Kero,[6,7] Hendrik Undeutsch,[7] Samuel Refetoff,[3,8,9] Kurt W. Schmid,[2] Dagmar Führer,[1] and Lars C. Moeller[1]

Background: Radioiodine refractory dedifferentiated thyroid cancer is a major clinical challenge. Anaplastic lymphoma kinase (ALK) mutations with increased ALK activity, especially fusion genes, have been suggested to promote thyroid carcinogenesis, leading to development of poorly differentiated thyroid carcinoma (PDTC) and anaplastic thyroid carcinoma. To determine the oncogenic potential of increased ALK activity in thyroid carcinogenesis *in vivo*, we studied mice with thyrocyte-specific expression of a constitutively active ALK mutant.
Methods: Mice carrying a Cre-activated allele of a constitutively active ALK mutant (F1174L) were crossed with mice expressing tamoxifen-inducible Cre recombinase ($CreER^{T2}$) under the control of the thyroglobulin (Tg) gene promoter to achieve thyrocyte-specific expression of the ALK mutant (ALK^{F1174L} mice). Survival, thyroid hormone serum concentration, and tumor development were recorded. Thyroids and lungs were studied histologically. To maintain euthyroidism despite dedifferentiation of the thyroid, a cohort was substituted with levothyroxine (LT4) through drinking water.
Results: ALK^{F1174L} mice developed massively enlarged thyroids, which showed an early loss of normal follicular architecture 12 weeks after tamoxifen injection. A significant decrease in Tg and Nkx-2.1 expression as well as impaired thyroid hormone synthesis confirmed dedifferentiation. Histologically, the mice developed a carcinoma resembling human PDTC with a predominantly trabecular/solid growth pattern and an increased mitotic rate. The tumors showed extrathyroidal extension into the surrounding strap muscles and developed lung metastases. Median survival of ALK^{F1174L} mice was significantly reduced to five months after tamoxifen injection. Reduced Tg expression and loss of follicular structure led to hypothyroidism with elevated thyrotropin (TSH). To test whether TSH stimulation played a role in thyroid carcinogenesis, we kept ALK^{F1174L} mice euthyroid by LT4 substitution. These mice developed PDTC with identical histological features compared with hypothyroid mice, demonstrating that PDTC development was due to increased ALK activity and not dependent on TSH stimulation.
Conclusion: Expression of a constitutively activated ALK mutant in thyroids of mice leads to development of metastasizing thyroid cancer resembling human PDTC. These results demonstrate *in vivo* that increased ALK activity is a driver mechanism in thyroid carcinogenesis.

Keywords: anaplastic lymphoma kinase, ALK, PDTC, poorly differentiated thyroid cancer

Introduction

Thyroid cancer is the most common endocrine malignancy. Differentiated thyroid carcinoma (DTC) accounts for ~90% of all thyroid cancers and shows an excellent prognosis. In contrast, poorly differentiated thyroid carcinoma (PDTC) and anaplastic thyroid carcinoma (ATC) are rare but have an unfavorable and often fatal prognosis (1–4). PDTC accounts for a small proportion of all thyroid cancers with marked geographical differences: whereas PDTC is rarely seen in Japan (0.3%) and the United States (1.8%), it accounts for 4–6% of all thyroid cancers in Europe and Latin America (5–7).

[1]Department of Endocrinology, Diabetes and Metabolism; [2]Institute of Pathology; [4]Clinic for Bone Marrow Transplants; University Hospital Essen, University of Duisburg-Essen, Essen, Germany.
Departments of [3]Medicine and [8]Pediatrics; [9]Committee on Genetics; The University of Chicago, Chicago, Illinois.
[5]Pediatric Oncology and Hematology, Charité University Medicine, Berlin, Germany.
[6]Department of Pediatrics and [7]Research Centre for Integrative Physiology and Pharmacology, Turku Center for Disease Modeling, Institute of Biomedicine, University of Turku, Turku, Finland.
*Contributed equally.

The tumors are usually widely invasive, extending to perithyroidal soft tissues in 60–70%. Regional lymph node involvement is found in 15–65%, and distant metastases, most commonly to the lung, are reported in 40–70% (5–10). The overall 5-year survival of patients with PDTC is 60–70% and the 1-year survival of ATC is 10–20% (11). The poor prognosis is attributable to early mutations, the invasive and aggressive nature of the cancers, and, usually, refractoriness to radioiodine (3,12,13). Therefore, a main effort in thyroid cancer research is the identification of driver mutations in aggressive thyroid cancer amenable to targeted therapy (12,14,15).

A novel promising protein for targeted therapy could be the anaplastic lymphoma kinase (ALK). Oncogenic potential of ALK was first identified in neuroblastoma and nonsmall cell lung cancer (16–18). A potential pathogenic role for ALK in development of thyroid cancer is based on the recent findings of ALK fusion genes in thyroid cancer without known driver mutations, for example, BRAF, RAS, or RET/PTC rearrangements.

Fusions of striatin (*STRN*), echinoderm microtubule-associated protein-like 4 (*EML4*), or Coiled-Coil Domain Containing 149 (*CCDC149*) genes with the kinase domain of the *ALK* gene were found in thyroid cancer samples (12,14,19–21). In large-scale genetic studies, 4 *ALK* fusions were detected in 256 papillary thyroid carcinomas (PTCs), 3 in 35 PDTCs and 1 in 24 ATCs (14), 3 in 84 PDTCs and none in 33 ATCs (12), and 2 in 468 adult PTCs and none in 196 ATCs (21). In addition to ALK fusions, activating ALK point mutations has been reported in ATC (4,15). Fusion genes lead to increased expression and activity of the ALK. Consequently, expression of STRN-ALK transformed cells *in vitro* and induced tumor formation in subcutaneous rat PCCL3 cell xenografts (14).

The potential of ALK fusions to transform cells and the lack of overlap with other driver mutations in thyroid cancer samples suggested that increased ALK activity is an independent driver event in the development of thyroid cancer. To determine whether increased ALK activity is an independent driver event for thyroid cancer *in vivo*, we studied mice with thyrocyte-specific expression of the constitutively active ALK mutant F1174L (17,22). These mice develop an aggressive thyroid carcinoma with loss of follicular architecture and hormone synthesis, strap muscle invasion, and lung metastases, resembling human PDTC.

Materials and Methods

Animals and treatment

All animal experiments were approved by the Landesamt für Natur, Umwelt und Verbraucherschutz (LANUV) of North Rhine-Westphalia, Germany. A constitutively active ALK mutant (F1174L) was cloned into the Rosa26 locus. Expression of this ALK mutant is prevented by an upstream element containing a stop codon and a poly-A tail (hGH-pA; Supplementary Fig. S1A). This element is flanked by loxP sites (lox-stop-lox model). After excision of this stop element by Cre recombinase, expression of the ALK^{F1174L} mutant is driven by the synthetic CAG promoter (17). In addition, the ALK^{F1174L} transgene also encodes for luciferase downstream from an internal ribosomal entry site (IRES).

To achieve thyrocyte-specific expression of ALK^{F1174L}, heterozygous ALK^{F1174L} mice ($ALK^{F1174L/+}$) were crossed with mice expressing Cre recombinase under control of a tamoxifen-inducible thyroglobulin promoter ($TgCreER^{T2+/0}$) (23) (Supplementary Fig. S1A). $TgCreER^{T2+/0}$;$ALK^{F1174L/+}$ are referred to as ALK^{F1174L} mice, and $TgCreER^{T2+/0}$;$ALK^{+/+}$ were used as controls, referred to as wild type (WT) mice. The background strain was C57BL/6. Mice were housed at 21°C ± 1°C and an alternating 12-hour light and 12-hour dark cycle. Standard chow (Sniff, Soest, Germany) and tap water were provided *ad libitum*, unless otherwise indicated. Tamoxifen was dissolved in corn oil (Sigma-Aldrich, St. Louis) at a concentration of 30 mg/mL.

At the age of 4–7 weeks and a body weight >15 g, ALK^{F1174L} mice as well as WT littermates were injected intraperitoneally (i.p.) with 3 mg tamoxifen in 100 μL per mouse per day for 5 consecutive days (Supplementary Fig. S1A, B). Levothyroxine (LT4) substitution started 1 week after the first tamoxifen injection with tap water containing 133 ng/mL LT4 (renewed 3 times per week). LT4 stock solution was prepared at a concentration of 5 mg LT4 per 50 mL, 40 mM NaOH, and 0.2% bovine serum albumin (BSA) and stored in the dark at −20°C. The drinking water contained 130 ng/mL thyroxine (T4). Total T4 (TT4) serum concentrations in mice were measured every 30 days.

Genotyping and detection of recombination

Mice were genotyped using a standardized polymerase chain reaction (PCR) program and primers as follows: ALK^{F1174L}-KI-rev 5′-CCCAAGGCACACAAAAAACC-3′, ALK^{F1174L}-KI-fwd 5′-TGGCAGTCTAGGATCTG-3′, Cre-ERT2-rev 5′-TGGCAGCTCTCATGTCTCCAG-3′, Cre-ERT2-fwd 5′-TCAGAGATACCTGGCCTGGTC-3′. All primers were purchased from Eurofins MWG Operon (Ebersberg, Germany). Initial denaturation at 95°C for 5 minutes was followed by 40 cycles of 95°C for 30 seconds, 60°C for 15 seconds, and 72°C for 35 seconds. A final elongation step was carried out at 72°C for 3 minutes. Successful thyrocyte-specific Cre-mediated recombination was confirmed by PCR with the following primers: mALK-recom-rev: 5′- GCA CCA CGA AGT CAA CTG C -3′, ALK^{F1174L}-fwd: 5′-TGG CAG TC TAG GAT CTG-3′, Rosa26-wt-rev: 5′-CAT GTC TTT AAT CTA CCT CGA TGG -3′; Rosa26-wt-fwd: 5′-CTC TTC CCT CGT GAT CTG CAA CTC C -3′(Supplementary Fig. S2).

In vivo *bioluminescence imaging*

ALK expression was also determined by detection of the coupled luciferase expression by *in vivo* imaging. Luciferase expression was coupled to ALK^{F1174L} expression through an IRES. Mice were anesthetized with 1.75–2.5% isoflurane followed by an i.p. injection of 150 μg/g D-luciferin (Perkin Elmer, Massachusetts) dissolved in phosphate-buffered saline (PBS). Five minutes after injection, mice were imaged in an IVIS Lumina II imaging system (Perkin Elmer). Changes in bioluminescence intensity over time were measured and are presented as total flux values in photons per second. The total flux was calculated in regions of interest on each mouse with Living Image 4.1 acquisition and analysis software (Perkin Elmer) (Binning: 4, FOV 12.5, exposure time 1 second).

Histology and immunostaining

Mice were euthanized with CO_2 when predefined criteria were met, for example, loss of weight (≥20% body weight) or significant difficulty of breathing. A separate cohort of mice was euthanized at certain time points with CO_2 to investigate cancer development. Blood was collected by cardiac puncture and serum was prepared as described previously (24). Directly after dissection, thyroid gland, brain, lung, and liver of each animal were macroscopically evaluated. Tissues were then fixed in 4% paraformaldehyde (phosphate buffered) and embedded in paraffin. Normal thyroid as well as tumor morphology was analyzed on 5-μm thick sections obtained from paraffin-embedded tissues stained with hematoxylin and eosin.

For Nkx-2.1 immunohistochemistry, endogenous peroxidases in thyroid sections were blocked with 3% hydrogen peroxide for 5 minutes. The primary antibody (1:50, Nkx-2.1, MA5-13961; Thermo Fisher Scientific, Inc., Waltham) was incubated for 30 minutes. The slides were incubated with horseradish peroxidase-labeled antimouse IgG for 30 minutes, 10 minutes with ZytoDAB, followed by hematoxylin (1:8; 5 minutes) staining. The samples were fixed with Immu-Mount (Thermo Fisher Scientific, Inc.). Tg and vimentin (Vim) expression was analyzed by immunofluorescence. Samples were blocked with 3% BSA/0.1% Triton/PBS for 30 minutes at room temperature (RT).

Samples were incubated with primary antibodies for Tg (1:1000, ab156008; Abcam) and Vim (1:100, D21H3; Cell Signaling, Danvers) dissolved in 1% BSA/0.1% Triton/PBS overnight at 4°C in a humidified chamber and protected from light. Appropriate Cy3-labeled secondary antibodies were dissolved in 1% BSA/PBS (1:200). Samples were then incubated with a secondary antibody for 1 hour at RT. Sections were counterstained with Hoechst 33342 (1:1000 in PBS; Thermo Fisher Scientific, Inc.) for 5 minutes at RT to visualize nuclei. Images were taken with an ELYRA PS.1 LSM710 confocal microscope (Zeiss, Germany). Pseudocolor imaging (green) was used to visualize Tg.

Mouse thyroid sections were reviewed by two experienced thyroid pathologists blinded to the genotype. For detection of Ki-67, tissue sections were incubated with a rabbit anti-Ki-67 antibody (1:400, RBK027; Zytomed Systems, Germany) and positivity was detected with the ZytoChem-Plus HRP Kit (ZytoChem-Plus HRP Kit, Broad Spectrum; HRP008DAB; Zytome Systems, Germany). A total of 500–1000 tumor cells were counted from 10 representative images of each stained tumor. Ki-67 index was calculated by dividing Ki67-positive by Ki67-negative epithelial cells.

Immunoblot analysis

Thyroid tissues (WT thyroids $n = 2$, ALK^{F1174L} thyroids $n = 2$) were homogenized in radioimmunoprecipitation assay lysis buffer (150 mM NaCl, 50 mM Tris–HCl, 1% NP-40, 0.5% sodiumdesoxycholate, 0.1% sodium dodecyl sulfate (SDS), 2 mM ethylenediaminetetraacetic acid) with PhosSTOP and cOmplete Protease Inhibitor Cocktail (Sigma-Aldrich) for whole protein lysates. A total of 20 μg of protein were separated by SDS-polyacrylamide gel electrophoresis and blotted onto a polyvinyl difluoride membrane (Roti-Fluoro PVDF; Roth). Membranes were blocked with 5% BSA (Sigma-Aldrich) in Tris-buffered saline with 150 mM NaCl, 0.1% Tween 20, and pH 7.4 for 1 hour at RT.

The following primary antibodies were used: p44/42 MAPK (Erk1/2) (1:1000, #4695S; Cell Signaling), phospho-p44/42 MAPK (1:1000, #4370T; Cell Signaling), phospho-AKT (S473) (1:1000, #9271S; Cell Signaling), phospho-AKT (T308) (1:1000, #2965S; Cell Signaling), and AKT (1:1000, #9272; Cell Signaling). They were incubated overnight at 4°C. Antirabbit IgG HRP linked (1:2000; #7074S Cell Signaling) served as second antibody. The signals were detected with a VersaDocMP4000 (BioRad) and the band densities were determined with Image Lab software (BioRad).

Thyroid function tests

Serum thyrotropin (TSH) was measured with a sensitive heterologous disequilibrium double-antibody precipitation radioimmunoassay (25). TT4 was measured by ELISA (DRG Instruments, Marburg, Germany).

Statistical analyses

Data were analyzed with GraphPad Prism6. Data are presented as mean ± standard error of the mean unless otherwise specified. $p < 0.05$ was considered statistically significant.

Results

Thyroid-specific ALK^{F1174L} expression in $ALK^{F1174L/+}$ mice

Tamoxifen-inducible Tg-specific Cre mice ($Tg\text{-}CreERt^{+/0}$) were crossed with heterozygous lox-stop-lox $ALK^{F1174L/+}$ mice to generate heterozygous Tg-specific Cre mice either heterozygous for mutant ALK^{F1174L} ($Tg\text{-}CreERt^{+/0}$; $ALK^{F1174L/+}$) or homozygous for WT ALK ($Tg\text{-}CreERt^{+/0}$; $ALK^{+/+}$) (Supplementary Fig. S1A). To induce expression of the mutant ALK allele, ALK^{F1174L} mice were injected with tamoxifen (Supplementary Fig. S1B). WT littermates expressing Tg-specific Cre were also injected.

No transgene effect was observed without tamoxifen injections, and activation of Cre by tamoxifen in WT littermates did not affect thyroid morphology or function. In addition, we used *in vivo* imaging of tamoxifen-injected ALK^{F1174L} and WT mice, as an IRES genetically couples luciferase expression to ALK^{F1174L} expression. A bioluminescence signal was detected only in thyroids of tamoxifen-injected ALK^{F1174L} mice but not in WT mice (Supplementary Fig. S1C). Successful and thyrocyte-specific recombination was confirmed by PCR (Supplementary Fig. S2).

Thyrocyte-specific ALK^{F1174L} expression leads to development of thyroid tumors resembling human PDTC

ALK^{F1174L} mice developed massive goiters, which could be monitored *in vivo* by bioluminescence imaging (Fig. 1A). Goiters reached a volume up to 20-fold larger than that of WT thyroids with an irregular structure (Fig. 1B). This massive thyroid growth is probably the first consequence of constitutive activation of ALK and, subsequently, the MAPK/ERK and PI3K/AKT signaling pathways. Compared with thyroids from WT mice, thyroids from ALK^{F1174L} mice showed increased phosphorylation of ERK and AKT at T308, but not at S473 (Fig. 1C). Histologically, ALK^{F174L} thyroids showed

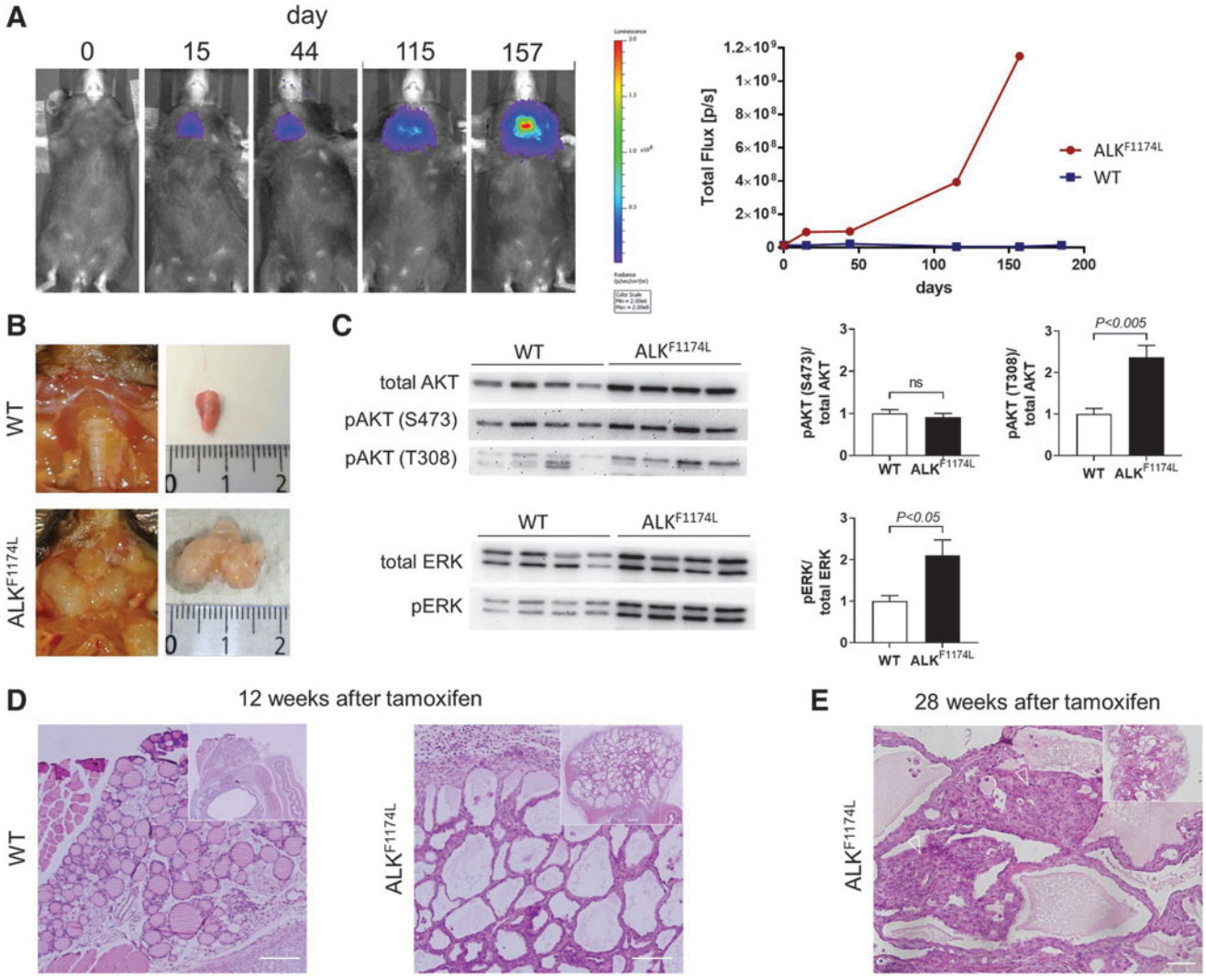

FIG. 1. Features of ALK^{F1174L}-positive thyroid glands. (**A**) Longitudinal quantification of bioluminescent signals in WT and ALK^{F1174L} mice. Pseudocolor images of one representative ALK^{F1174L} mouse (left). Signal intensity was quantified and is shown as a function of the number of days after injection of tamoxifen (right). (**B**) WT thyroid (top) compared with an enlarged ALK^{F1174L} thyroid (bottom) 43 weeks after tamoxifen induction. (**C**) PI3K/AKT and MAPK/ERK signaling pathway activation was determined by immunoblotting (left panel) and densitometry (right panel), normalized for total ERK and total AKT, respectively ($n=4$, mean ± SEM, t-test). (**D**) Compared with a WT thyroid (left), HE staining showed changes in follicular architecture in an ALK^{F1174L} thyroid (right) 12 weeks after tamoxifen treatment (inlets, overview of a whole thyroid lobe; scale bar = 100 μm). (**E**) Solid proliferates between follicles (open triangles) in ALK^{F1174L} thyroids (scale bar = 50 μm; inlet, overview of a whole thyroid lobe). HE, hematoxylin and eosin; SEM; WT, wild type.

partial follicular destruction and an increased number of perifollicular fibroblasts 12 weeks after tamoxifen injection.

Furthermore, numerous follicles showed a considerable reduction or complete lack of colloid (Fig. 1D). Twenty-eight weeks after tamoxifen injection, the thyroids of ALK^{F1174L} mice developed epithelial tumors with a solid/trabecular pattern (Fig. 1E). The tumor cell nuclei showed raisin-like folding of the nuclear membrane, resembling ''convoluted nuclei'' of human PDTC (8). Occasionally, mitotic figures were found, and the mitotic rate was >4/10 high power fields (HPF). Overall, the animal tumor morphology with a solid/trabecular growth pattern, convoluted tumor cell nuclei, and increased mitotic rate (>4/10 HPF) resembled human PDTC, meeting the so-called Turin consensus proposal criteria of PDTC (8), which have been included as an integral part of the PDTC definition in the recently published WHO classification of thyroid gland tumors (11).

Loss of thyroid-specific markers confirms dedifferentiation of thyrocytes

In contrast to thyroids from WT mice, which showed homogeneous Tg staining (Fig. 2A, left), ALK^{F1174L} thyroids displayed partial loss of Tg staining (Fig. 2A, right). The tumors showed, similar to human PDTCs, a significantly reduced Tg expression. Similarly, decreasing expression of Nkx-2.1 demonstrated the gradual dedifferentiation of thyrocytes (26). Whereas WT thyroids were positive for Nkx-2.1 in

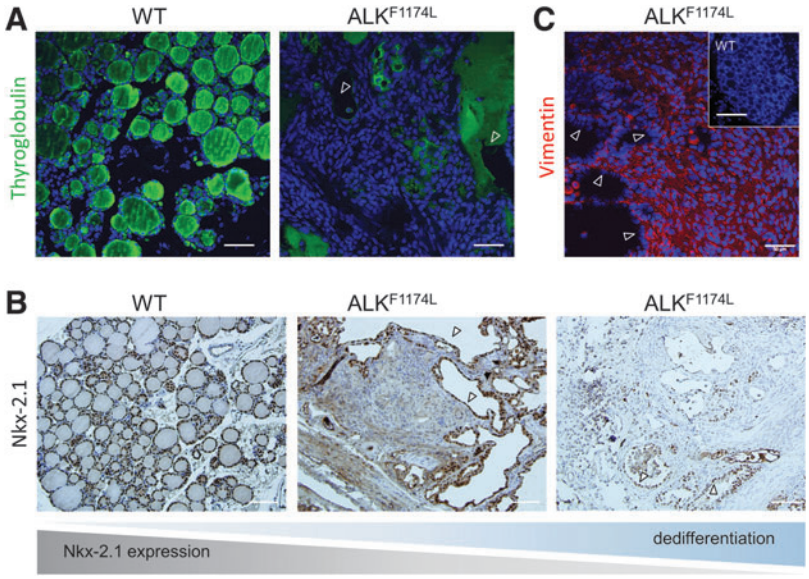

FIG. 2. Loss of thyroid-specific differentiation markers and signaling pathway activation in ALK^{F1174L} thyroids. (**A**) Expression of Tg (green) was determined by immunofluorescence staining and confocal microscopy in WT and ALK^{F1174L} thyroids. Open triangles indicate follicles negative for Tg or showing a weak expression compared with WT follicles (left) (scale bar = 50 μm; blue; nuclei, counterstained with Hoechst 33342). (**B**) Staining for Nkx-2.1 revealed a distinct decrease of nuclear Nkx-2.1 expression in thyroids of ALK^{F1174L} mice over time (middle and right) compared with WT thyroids (left). Residual Nkx-2.1 expression was detected in follicle-forming thyrocytes (triangles) but not in stroma cells (scale bar = 100 μm; nuclei were counterstained with hematoxylin). (**C**) WT thyroids were completely negative for Vim staining (inlet; scale bar = 300 μm). ALK^{F1174} expressing thyroids displayed an increased Vim staining (red) of stroma cells. Follicle-forming thyrocytes were still negative for Vim expression (open triangles). Tg, thyroglobulin; Vim, vimentin.

almost all follicular cells, Nkx-2.1 expression in ALK^{F1174L} thyroids was severely diminished 28 weeks after tamoxifen injection and even further reduced with increasing animal age (Fig. 2B). In ALK^{F1174L}-positive mice, Nkx-2.1 positivity was only preserved in the few follicle-forming thyrocytes.

Cancer aggressiveness is particularly enhanced by endothelial–mesenchymal transition (EMT) that allows a polarized epithelial cell to undergo phenotypical changes, enabling it to assume a mesenchymal cell phenotype, including an augmented migratory capacity (27,28). We, therefore, analyzed EMT by staining sections from ALK^{F1174L} thyroids for Vim, a protein of the cytoskeleton of mesenchymal cells and a specific marker for EMT (27,28). Although WT thyroid sections were completely negative for Vim staining, the number of Vim-expressing cells was increased in ALK^{F1174L} thyroids (Fig. 2C). This finding confirms EMT and supports the ALK-driven dedifferentiation of thyroid tissue.

Thyroid-specific ALK^{F1174L} expression leads to development of an aggressive metastatic thyroid carcinoma

To evaluate tumor aggressiveness, we analyzed thyroid sections from ALK^{F1174L} mice for signs of local invasion and screened peripheral organs (lung, liver, and brain) for metastases. We found invasive tumor infiltrating the surrounding cervical strap muscle tissue (Fig. 3A). The high mitotic rate of the PDTC-like tumors was confirmed by a Ki67 positivity of 26% (Fig. 3B). In addition to local invasive tumor growth, the tumors developed lung metastases (Fig. 3C).

Of note, lung metastases occurred as early as 24 weeks after tamoxifen treatment in ALK^{F1174L} mice. The lung metastases showed morphological similarity to the primary tumor with a solid/trabecular growth pattern, convoluted tumor cell nuclei, and an increased mitotic rate (Fig. 3D, E). No metastases were found in brain and liver. The aggressive behavior of the ALK^{F1174L}-dependent thyroid carcinomas was associated with a severely reduced survival of ALK^{F1174L} mice. Whereas all WT mice survived the observation period of 60 weeks without complications, the median survival of ALK^{F1174L} mice was severely reduced to only 20 weeks after tamoxifen injection.

Hypothyroidism is not a prerequisite for thyroid cancer development, but appears to promote progression

Considering the loss of follicular structure as well as the apparent dedifferentiation of ALK^{F1174L} thyroids, we tested whether thyroid hormone synthesis was impaired. TT4 serum concentrations were significantly decreased in ALK^{F1174L} mice compared with WT mice (Fig. 4). Consequently, the TSH serum concentration was severely increased in ALK^{F1174L} mice (Fig. 4). In summary, destruction of the follicular structure and dedifferentiation led to overt hypothyroidism in ALK^{F1174L} mice. TSH stimulates thyrocyte and thyroid cancer growth.

To test whether stimulation by TSH is required for thyroid cancer development in ALK^{F1174L} mice, we directly compared ALK^{F1174L} mice with and without LT4 substitution through drinking water starting at the time point of the tamoxifen injections. LT4 substitution prevented development of hypothyroidism and the mice remained euthyroid with unchanged

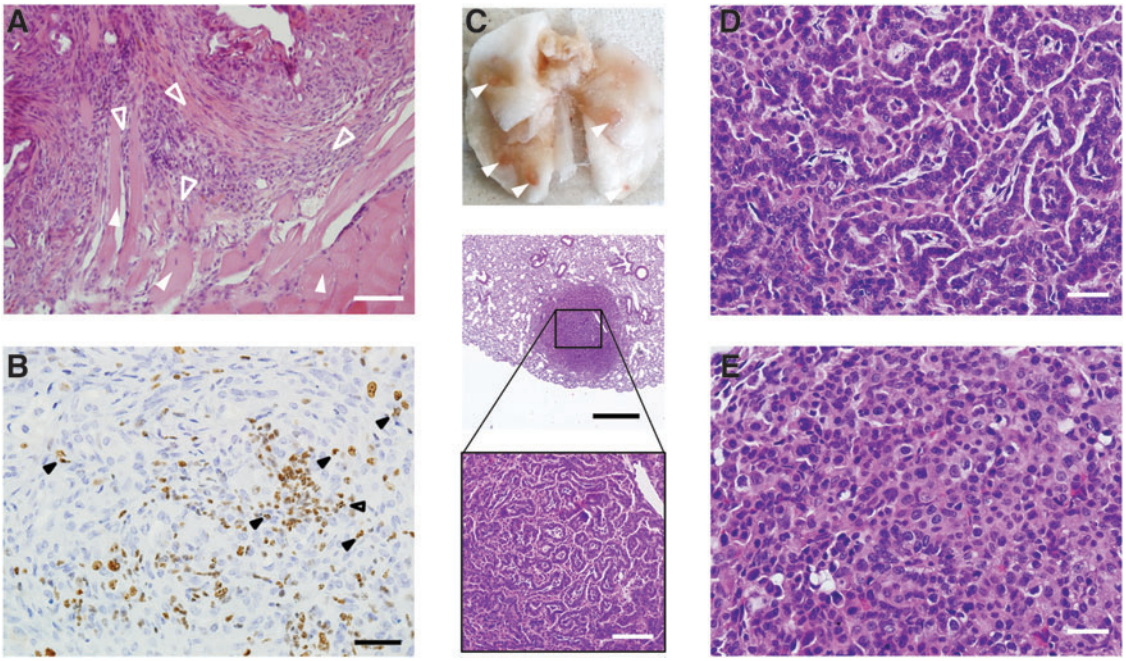

FIG. 3. Invasive growth and pulmonary metastasis of PDTC-like thyroid tumors. (**A**) PDTC-like thyroid tumors of ALK^{F1174L} mice show invasion (open triangles) into the surrounding strap muscles (solid triangles) (HE staining, 52 weeks after tamoxifen injection; scale bar = 100 μm). (**B**) Ki67 staining confirmed a high proliferation rate, mitotic events (open triangle), and convoluted nuclei (closed triangle) in ALK^{F1174L} thyroids (42 weeks after tamoxifen injection; scale bar = 50 μm). (**C**) Macroscopic aspect of an ALK^{F1174L} lung with tissue abnormalities (triangles; upper panel). Microscopy confirmed lung metastases with PDTC-like trabecular morphology (HE staining; middle and lower panel; black scale bar = 200 μm; white scale bar = 50 μm). (**D**) Different lung metastases with trabecular structure or (**E**) with a more solid growth pattern. Both metastases were found in the same animal (42 weeks after tamoxifen injection; scale bar = 20 μm). PDTC, poorly differentiated thyroid carcinoma.

TT4 throughout the experiment (Supplementary Fig. S3). These animals developed thyroid cancers with identical histological features as mice without LT4 substitution. The median survival was longer in mice on LT4 substitution (32 vs. 18 weeks, $p < 0.001$; Fig. 5), whereas the final tumor weight did not differ between the 2 groups (375 ± 204 mg without LT4 vs. 449 ± 237 mg with LT4, not significant).

Thus, also in euthyroid mice, increased ALK activity is sufficient to induce thyroid cancer, whereas hypothyroidism with increased TSH stimulation appears to promote tumor progression.

Discussion

ALK mutations and gene rearrangements have been described in PTC, PDTC, and ATC (12,14,15). Because ALK fusions increase cell proliferation and transformation *in vitro* and in xenografts, increased ALK activity is considered a driver mechanism for thyroid cancer development. We studied whether increased ALK activity with subsequently increased PI3K and MAPK/ERK signaling in thyrocytes leads to development of thyroid cancers *in vivo* and, if so, which type of cancer. Increased thyrocyte-specific expression of a constitutively ALK mutant in ALK^{F1174L} mice led to the development of thyroid cancers with features closely resembling human PDTC.

The pathogenic potential of ALK fusion genes depends on two main features, increased expression and ligand-independent ALK activation. Whereas WT ALK expression in thyrocytes is low, expression of the *STRN-ALK* and *EML4-ALK* fusion genes is significantly higher, on average 55-fold that of WT ALK (14,29), due to the active promoter of

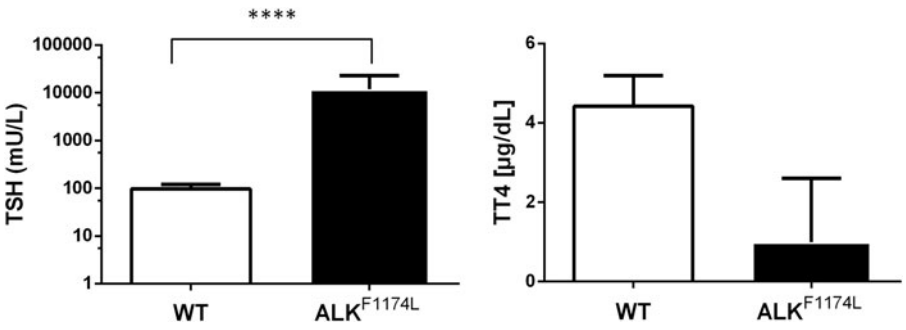

FIG. 4. Thyroid-specific ALK^{F1174L} expression leads to overt hypothyroidism. Serum concentration of TT4 was significantly decreased in ALK^{F1174L} mice (black column) compared with WT control mice (open column). A significantly higher serum concentration of TSH in ALK^{F1174L} mice confirmed hypothyroidism. (WT $n = 5$ and ALK^{F1174L} $n = 13$; unpaired *t*-test). TSH, thyrotropin; T4, thyroxine; TT4, total T4.

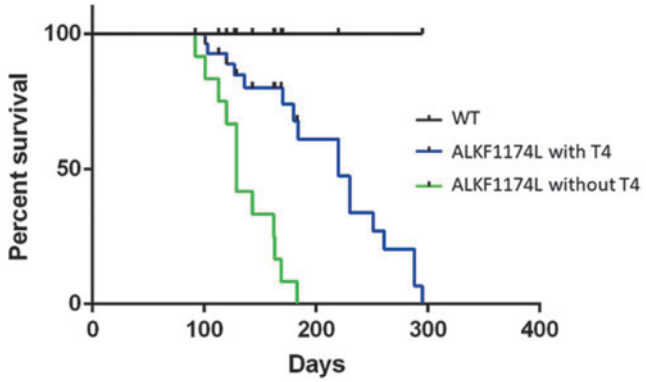

FIG. 5. Median survival is reduced in ALK^{F1174L} mice. Kaplan–Meier analysis of ALK^{F1174L} without ($n=12$) and with ($n=17$) T4 substitution and WT ($n=13$ with and without [$n=14$] T4 substitution) mice shows a severely reduced median survival of ALK^{F1174L} mice to 18 weeks after induction of ALK^{F1174L} expression through tamoxifen, whereas all WT mice survived the observation period. Compared with untreated mice, substitution with T4 lead to a significantly longer survival (32 weeks, $p<0.001$).

the upstream fusion partner. The upstream fusion partner also provides a dimerization domain that leads to ligand-independent activation of the ALK domain and increased signaling with increased MAPK activation.

In the mouse model used here, the mechanism of increased expression and activity of ALK differs from fusion genes. First, in *STRN-ALK* and *EML4-ALK* fusion genes, the active promoter that increases expression of the chimeric gene is provided by the upstream fusion partner, whereas in the ALK^{F1174L} mouse an active synthetic promoter ensures increased ALK expression. Second, in STRN-ALK fusion proteins, ligand-independent ALK activation is mediated by a dimerization domain provided by the upstream fusion partner, whereas in the ALK^{F1174L} mouse, an activating mutation leads to ligand-independent ALK activation. Notwithstanding these mechanistic differences between mouse model and patients, the ALK^{F1174L} mouse demonstrates *in vivo* that increased ALK activity with subsequent MAPK and PI3K signaling pathway activation is a driving event in development of thyroid cancer, with a phenotype consistent with PDTC.

According to the WHO classification (11), human PDTC is defined as a follicular cell neoplasm that shows limited evidence of follicular cell differentiation and is morphologically and behaviorally intermediate between differentiated (follicular and papillary) and anaplastic carcinomas. The histopathological criteria for PDTC, as listed in the Turin consensus proposal (8), are a solid, trabecular, and/or insular growth pattern, convoluted tumor cell nuclei, tumor necrosis, and/or an increased mitotic rate (>3/10 HPF).

Furthermore, human PDTC shows decreased expression of Tg, diminished expression of Nkx-2.1, and a Ki67 index of 10–30% (11). The thyroid tumors of ALK^{F1174L} mice showed a solid/trabecular growth pattern, convoluted nuclei, an increased mitotic rate, reduced Tg and Nkx-2.1 expression, a high Ki67 index and extrathyroidal extension into cervical strap muscles and lung metastases. Thus, the thyroid carcinomas found in ALK^{F1174L} mice meet the criteria developed for the diagnosis of human PDTC.

Dedifferentiation with reduced Tg expression and loss of the regular follicular structure led to severe hypothyroidism and a significant increase in TSH in ALK^{F1174L} mice. TSH is a stimulus of thyroid cancer growth. Such a stimulatory effect of TSH had been demonstrated in $TR\beta^{PV/PV}$ mice that develop PTC only when thyrotropin receptor signaling is intact (30). In contrast, hypothyroidism alone for more than a year leads to thyroid growth in WT mice, but not to development of metastatic thyroid cancer. These observations led to the conclusion that stimulation of growth by TSH is necessary but not sufficient for PTC development. Similarly, in thyroid-specific $BRAF^{V600E}$ mice, complete TSH receptor knockout appeared to attenuate PTC development but did not prevent it (31,32). Euthyroid $BRAF^{V600E}$ mice still developed PTC (33).

These mouse models suggest that the presence of an oncogenic mutation is a prerequisite for development of thyroid cancer, while additional stimulation by TSH may promote cancer progression. Our results are in agreement with this hypothesis. Hypothyroid as well as LT4-substituted ALK^{F1174L} mice developed PDTC, demonstrating that PDTC development is due to expression of the constitutively active ALK mutant and not to prolonged TSH stimulation. Yet, the survival time was reduced in hypothyroid mice, indicating that TSH stimulation does promote thyroid cancer growth.

Increased ALK activity, mainly due to ALK fusion genes, had been suggested as a driving event in the development of dedifferentiated thyroid carcinoma. The development of PDTC in the mouse model with increased ALK activity presented here strongly supports this hypothesis with *in vivo* data.

Author Disclosure Statement

No competing financial interests exist.

Funding Information

This study was supported by a young investigator grant to H.K. (Stiftung Universitätsmedizin Essen) and Mercator Research Center Ruhr (An-2015-0054) and Deutsche Forschungsgemeinschaft (Mo 1018/3-1) grants to L.C.M.

Supplementary Material

Supplementary Figure S1
Supplementary Figure S2
Supplementary Figure S3

References

1. Schmidbauer B, Menhart K, Hellwig D, Grosse J 2017 Differentiated thyroid cancer-treatment: state of the art. Int J Mol Sci **18:** pii: E1292.
2. Haugen BR, Sawka AM, Alexander EK, Bible KC, Caturegli P, Doherty GM, Mandel SJ, Morris JC, Nassar A, Pacini F, Schlumberger M, Schuff K, Sherman SI, Somerset H, Sosa JA, Steward DL, Wartofsky L, Williams MD 2017 American Thyroid Association Guidelines on the Management of Thyroid Nodules and Differentiated Thyroid Cancer Task Force Review and Recommendation on the proposed renaming of encapsulated follicular variant papillary thyroid carcinoma without invasion to noninvasive follicular thyroid neoplasm with papillary-like nuclear features. Thyroid **27:**481–483.

3. Smallridge RC, Ain KB, Asa SL, Bible KC, Brierley JD, Burman KD, Kebebew E, Lee NY, Nikiforov YE, Rosenthal MS, Shah MH, Shaha AR, Tuttle RM, American Thyroid Association Anaplastic Thyroid Cancer Guidelines T 2012 American Thyroid Association guidelines for management of patients with anaplastic thyroid cancer. Thyroid **22:**1104–1139.
4. Xing M 2013 Molecular pathogenesis and mechanisms of thyroid cancer. Nat Rev Cancer **13:**184–199.
5. Carcangiu ML, Zampi G, Rosai J 1984 Poorly differentiated (''insular'') thyroid carcinoma. A reinterpretation of Langhans' ''wuchernde Struma''. Am J Surg Pathol **8:** 655–668.
6. Gnemmi V, Renaud F, Do Cao C, Salleron J, Lion G, Wemeau JL, Copin MC, Carnaille B, Leteurtre E, Pattou F, Aubert S 2014 Poorly differentiated thyroid carcinomas: application of the Turin proposal provides prognostic results similar to those from the assessment of high-grade features. Histopathology **64:**263–273.
7. Asioli S, Erickson LA, Righi A, Jin L, Volante M, Jenkins S, Papotti M, Bussolati G, Lloyd RV 2010 Poorly differentiated carcinoma of the thyroid: validation of the Turin proposal and analysis of IMP3 expression. Mod Pathol **23:** 1269–1278.
8. Volante M, Collini P, Nikiforov YE, Sakamoto A, Kakudo K, Katoh R, Lloyd RV, LiVolsi VA, Papotti M, Sobrinho-Simoes M, Bussolati G, Rosai J 2007 Poorly differentiated thyroid carcinoma: the Turin proposal for the use of uniform diagnostic criteria and an algorithmic diagnostic approach. Am J Surg Pathol **31:**1256–1264.
9. Hiltzik D, Carlson DL, Tuttle RM, Chuai S, Ishill N, Shaha A, Shah JP, Singh B, Ghossein RA 2006 Poorly differentiated thyroid carcinomas defined on the basis of mitosis and necrosis: a clinicopathologic study of 58 patients. Cancer **106:**1286–1295.
10. Ibrahimpasic T, Ghossein R, Carlson DL, Nixon I, Palmer FL, Shaha AR, Patel SG, Tuttle RM, Shah JP, Ganly I 2014 Outcomes in patients with poorly differentiated thyroid carcinoma. J Clin Endocrinol Metab **99:**1245–1252.
11. Lloyd RO RY, Klöppel G, Rosai J 2017 WHO Classification of Tumours of Endocrine Organs. Volume 10. 4th Edition. International Agency for Research on Cancer, Lyon, France.
12. Landa I, Ibrahimpasic T, Boucai L, Sinha R, Knauf JA, Shah RH, Dogan S, Ricarte-Filho JC, Krishnamoorthy GP, Xu B, Schultz N, Berger MF, Sander C, Taylor BS, Ghossein R, Ganly I, Fagin JA 2016 Genomic and transcriptomic hallmarks of poorly differentiated and anaplastic thyroid cancers. J Clin Invest **126:**1052–1066.
13. Smallridge RC, Copland JA 2010 Anaplastic thyroid carcinoma: pathogenesis and emerging therapies. Clin Oncol (R Coll Radiol) **22:**486–497.
14. Kelly LM, Barila G, Liu P, Evdokimova VN, Trivedi S, Panebianco F, Gandhi M, Carty SE, Hodak SP, Luo J, Dacic S, Yu YP, Nikiforova MN, Ferris RL, Altschuler DL, Nikiforov YE 2014 Identification of the transforming STRN-ALK fusion as a potential therapeutic target in the aggressive forms of thyroid cancer. Proc Natl Acad Sci U S A **111:**4233–4238.
15. Murugan AK, Xing M 2011 Anaplastic thyroid cancers harbor novel oncogenic mutations of the ALK gene. Cancer Res **71:**4403–4411.
16. Chen Y, Takita J, Choi YL, Kato M, Ohira M, Sanada M, Wang L, Soda M, Kikuchi A, Igarashi T, Nakagawara A, Hayashi Y, Mano H, Ogawa S 2008 Oncogenic mutations of ALK kinase in neuroblastoma. Nature **455:**971–974.
17. Heukamp LC, Thor T, Schramm A, De Preter K, Kumps C, De Wilde B, Odersky A, Peifer M, Lindner S, Spruessel A, Pattyn F, Mestdagh P, Menten B, Kuhfittig-Kulle S, Kunkele A, Konig K, Meder L, Chatterjee S, Ullrich RT, Schulte S, Vandesompele J, Speleman F, Buttner R, Eggert A, Schulte JH 2012 Targeted expression of mutated ALK induces neuroblastoma in transgenic mice. Sci Transl Med **4:**141ra191.
18. Soda M, Takada S, Takeuchi K, Choi YL, Enomoto M, Ueno T, Haruta H, Hamada T, Yamashita Y, Ishikawa Y, Sugiyama Y, Mano H 2008 A mouse model for EML4-ALK-positive lung cancer. Proc Natl Acad Sci U S A **105:** 19893–19897.
19. Efanov AA, Brenner AV, Bogdanova TI, Kelly LM, Liu P, Little MP, Wald AI, Hatch M, Zurnadzy LY, Nikiforova MN, Drozdovitch V, Leeman-Neill R, Mabuchi K, Tronko MD, Chanock SJ, Nikiforov YE 2018 Investigation of the relationship between radiation dose and gene mutations and fusions in post-chernobyl thyroid cancer. J Natl Cancer Inst **110:**371–378.
20. Perot G, Soubeyran I, Ribeiro A, Bonhomme B, Savagner F, Boutet-Bouzamondo N, Hostein I, Bonichon F, Godbert Y, Chibon F 2014 Identification of a recurrent STRN/ALK fusion in thyroid carcinomas. PLoS One **9:**e87170.
21. Pozdeyev N, Gay LM, Sokol ES, Hartmaier R, Deaver KE, Davis S, French JD, Borre PV, LaBarbera DV, Tan AC, Schweppe RE, Fishbein L, Ross JS, Haugen BR, Bowles DW 2018 Genetic analysis of 779 advanced differentiated and anaplastic thyroid cancers. Clin Cancer Res **24:**3059–3068.
22. George RE, Sanda T, Hanna M, Frohling S, Luther W, 2nd, Zhang J, Ahn Y, Zhou W, London WB, McGrady P, Xue L, Zozulya S, Gregor VE, Webb TR, Gray NS, Gilliland DG, Diller L, Greulich H, Morris SW, Meyerson M, Look AT 2008 Activating mutations in ALK provide a therapeutic target in neuroblastoma. Nature **455:**975–978.
23. Undeutsch H, Lof C, Offermanns S, Kero J 2014 A mouse model with tamoxifen-inducible thyrocyte-specific cre recombinase activity. Genesis **52:**333–340.
24. Engels K, Rakov H, Zwanziger D, Moeller LC, Homuth G, Kohrle J, Brix K, Fuhrer D 2015 Differences in mouse hepatic thyroid hormone transporter expression with age and hyperthyroidism. Eur Thyroid J **4:**81–86.
25. Pohlenz J, Maqueem A, Cua K, Weiss RE, Van Sande J, Refetoff S 1999 Improved radioimmunoassay for measurement of mouse thyrotropin in serum: strain differences in thyrotropin concentration and thyrotroph sensitivity to thyroid hormone. Thyroid **9:**1265–1271.
26. Charles RP, Silva J, Iezza G, Phillips WA, McMahon M 2014 Activating BRAF and PIK3CA mutations cooperate to promote anaplastic thyroid carcinogenesis. Mol Cancer Res **12:**979–986.
27. Knauf JA, Sartor MA, Medvedovic M, Lundsmith E, Ryder M, Salzano M, Nikiforov YE, Giordano TJ, Ghossein RA, Fagin JA 2011 Progression of BRAF-induced thyroid cancer is associated with epithelial-mesenchymal transition requiring concomitant MAP kinase and TGFbeta signaling. Oncogene **30:**3153–3162.
28. Kalluri R, Weinberg RA 2009 The basics of epithelial-mesenchymal transition. J Clin Invest **119:**1420–1428.
29. Uhlen M, Fagerberg L, Hallstrom BM, Lindskog C, Oksvold P, Mardinoglu A, Sivertsson A, Kampf C, Sjostedt

E, Asplund A, Olsson I, Edlund K, Lundberg E, Navani S, Szigyarto CA, Odeberg J, Djureinovic D, Takanen JO, Hober S, Alm T, Edqvist PH, Berling H, Tegel H, Mulder J, Rockberg J, Nilsson P, Schwenk JM, Hamsten M, von Feilitzen K, Forsberg M, Persson L, Johansson F, Zwahlen M, von Heijne G, Nielsen J, Ponten F 2015 Proteomics. Tissue-based map of the human proteome. Science **347:** 1260419.

30. Lu C, Zhao L, Ying H, Willingham MC, Cheng SY 2010 Growth activation alone is not sufficient to cause metastatic thyroid cancer in a mouse model of follicular thyroid carcinoma. Endocrinology **151:**1929–1939.
31. Orim F, Bychkov A, Shimamura M, Nakashima M, Ito M, Matsuse M, Kurashige T, Suzuki K, Saenko V, Nagayama Y, Yamashita S, Mitsutake N 2014 Thyrotropin signaling confers more aggressive features with higher genomic instability on BRAF(V600E)-induced thyroid tumors in a mouse model. Thyroid **24:**502–510.
32. Franco AT, Malaguarnera R, Refetoff S, Liao XH, Lundsmith E, Kimura S, Pritchard C, Marais R, Davies TF, Weinstein LS, Chen M, Rosen N, Ghossein R, Knauf JA, Fagin JA 2011 Thyrotrophin receptor signaling dependence of Braf-induced thyroid tumor initiation in mice. Proc Natl Acad Sci U S A **108:**1615–1620.
33. Charles RP, Iezza G, Amendola E, Dankort D, McMahon M 2011 Mutationally activated BRAF(V600E) elicits papillary thyroid cancer in the adult mouse. Cancer Res **71:** 3863–3871.

Address correspondence to:
Lars C. Moeller, MD
Department of Endocrinology, Diabetes and Metabolism
University Hospital Essen
University of Duisburg-Essen
Hufelandstraße 55
Essen 45147
Germany

E-mail: lars.moeller@uni-due.de